ISSN 1330-3651 (Print), ISSN 1848-6339 (Online) https://doi.org/10.17559/TV-20180829092302
Preliminary communication

Modeling and Simulation of Working Characteristics of Lithium Titanate Batteries for Emergency Power Transmission

Liwei ZHANG, Wenyan DONG, Yang YANG, Minghe SUN

Abstract: This paper presents a battery model applied to dynamic simulation software. The simulation model uses only the battery State-Of-Charge (SOC) as a state variable in order to avoid the algebraic loop problem. It is shown that this model, composed of a controlled voltage source in series with a resistance, can accurately describe the lithium titanate battery discharge process. The model's parameters can be easily extracted from the manufacturer's discharge curve. In this paper, it is actually applied to the self-starting system after the emergency stop of the EMU, the simulation model of the system is established by MATLAB/Simulink, and the ground test platform is used to simulate the actual working condition of EMU to complete the experimental verification. The results of both simulation and experiment proved that the scheme of battery self-shifting driven system is feasible and correct.

Keywords: lithium titanate battery; MATLAB simulation; self-shifting driven by battery

1 INTRODUCTION

On April 18, 2007, the Chinese railways achieved the sixth major speed increase. Since then, the speed of China's trains has entered a new height, China entered the era of rapid railroads. It achieved breakthroughs in nine core technologies and prepared China's high-speed rail technology, providing conditions for the next high-speed rail development. The sign of the sixth-large speed-up is the creation of 140 trains of the "Harmony" localized EMUs at speeds of 200 kilometers per hour and above [1]. In addition, the latest high-speed "Harmony" EMU train and the harmonious high-power locomotive on the line, making China's passenger transport capacity and cargo capacity have all experienced rapid growth [2].

For China's rapid economic development, the transport capacity cannot meet the transport needs of economic development. The rapid development of the train will undoubtedly promote the sound and rapid development of China's economy and society. However, when the trains of the Harmony EMU train pass through the train segment, the train car station, the over-phase and the parking station, they may stop in the no-power zone. In the absence of contact network power supply, it is impossible to rely on its own power to achieve free travel, seriously affecting the shunting and operating efficiency. Therefore, it is very important to study a cost-effective mobility plan for the development of China's railways.

The traditional car-moving technologies include shifting of locomotives, exchange of mobile equipment, and manual carts. These three types of vehicle-moving technologies have the disadvantages of high cost, low safety, and are easily causing environmental pollution and waste of personnel [3-5].

The battery itself is an integral part of the EMU and is generally used to provide power for the auxiliary power supply system. Therefore, the storage battery is very broad for the development of power supply, so it can also be used as a power source for the EMU emergency power failure.

The battery transfer technology uses the battery provided by the EMU as the power source to realize the low-speed walking off the train, which changes the traditional mode of diversion of the field and further reduces the cost of maneuvering and the waste of personnel, which is of great practical value. As shown in Fig. 1, it is a battery self-shifting driven system model topology. The direct boost of the battery provides power to the inverter and the motor, so battery selection and excellent performance are critical [6].

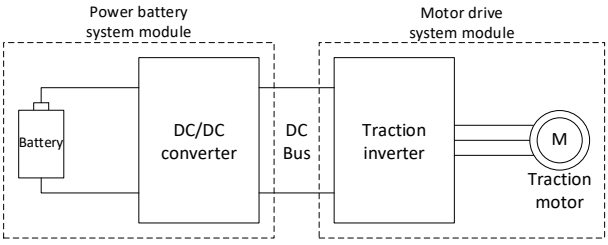

Figure 1 Battery self-shifting driven system model topology

2 DEVELOPMENT STATUS OF ELECTRIC VEHICLE AUXILIARY SYSTEM POWER SUPPLY BATTERIES

2.1 EMU Auxiliary Battery Selection Principle

The main function of the EMU-assisted battery pack is that the vehicle is used as an emergency backup power source to supply power to the vehicle's internal load and drive the vehicle to operate under the condition that the vehicle is driven through an electric train section, an EMU, and an over-equal non-contact network. When selecting EMU battery packs, the following principles are mainly followed [7-9]:

1) Light weight, adapt to the lightweight design concept of EMUs, achieve high safety and low energy consumption for vehicle operation.
2) Wide temperature adaptability, able to work stably at the ambient temperature of −40 - 60 °C.
3) Long life, long battery life, reduce battery replacement workload and operating costs.
4) The safety is good, the safety of the battery is high, and the safety of the vehicle operation can be effectively guaranteed.
5) The power characteristics are good, which can meet the need of high current charging and discharging of EMUs.
6) Others can adapt to the vibration requirements of EMUs when driving, low self-discharge, no

environmental pollution, no memory effect, good recycling and so on.

2.2 EMU Auxiliary Battery Pack Development Status

The existing batteries mainly include lead-acid batteries, nickel-cadmium batteries [10], sodium-sulfur batteries, and lithium-ion batteries. The main performance indicators of the battery include total cost, service life, power density, energy density, and efficiency. The characteristics of each power battery are shown in Tab. 1.

Table 1 Different power battery characteristics

Battery technology	Sodium-sulfur battery	Lead-acid battery	Nickel-chromium battery	Lithium battery
Total cost ($/kW·h)	245	170-250	300	90-155
Service life (cycle)	2500-4500	500-1500	1000-3500	1500-3500
Power density (W/kg)	300-450	200-300	150-350	250-450
Energy density (W·h/kg)	150-240	30-50	50-70	90-130
Effectiveness (%)	75-86	85	60-70	85-99

At present, there are two main types of auxiliary batteries for EMUs: one is a lead-acid battery, and the other is an alkaline nickel-cadmium battery. For a long time, lead-acid batteries have been widely used due to their mature technology, stable performance, and low price. However, because of its large weight and size, long charging time, and short life, lead-acid batteries are difficult to meet the requirements for efficient operation of modern EMUs. Compared with lead-acid batteries, nickel-cadmium batteries have good high-current discharge characteristics, high over-discharge resistance, and easy maintenance. They have been widely used in EMUs, but they have memory effects, low energy density, and the presence of heavy metals. Environmental pollution limits the continuous development of nickel-cadmium batteries.

Lithium-ion batteries are advanced batteries developed in the 1990s and are ideal sources of power in the future. The original lithium-ion battery was mainly composed of lithium cobalt oxide and showed obvious advantages in terms of energy density, power density, voltage platform, and lifespan. It was rapidly promoted and applied on portable devices. However, due to poor battery safety and longevity, irrational use will lead to a rapid decline in battery capacity. Abuse may cause smoke, fire, explosion, and other hidden dangers. Therefore, the application of medium-to-large power batteries has been restricted [11-12].

Battery researchers have introduced batteries of lithium manganate, ternary and lithium iron phosphate systems by improving the battery's positive electrode materials. The battery's safety and cycle life have been greatly improved, and it has been promoted in electric vehicles and other occasions application.

However, since carbon is used as a negative electrode in the above batteries, the ability of lithium to be inserted into and pulled out of the negative electrode is lowered under a low temperature environment, and in particular, the embedding capacity is decreased, so charging at a low temperature is more difficult than discharging, which affects the charge/discharge current of the battery. When the charging current is too large, the rate of lithium ions escaping from the positive electrode is greater than the negative electrode embedding rate, and lithium that cannot be embedded is deposited on the surface of the battery in the form of atomicity, which may lead to safety hazards of the battery.

In order to solve this problem, the battery researchers also conducted an in-depth study of the anode material of lithium-ion batteries, and introduced a lithium-ion battery with lithium titanate as a negative electrode—a lithium titanate battery. The battery in the case of a slight drop in battery energy density, battery temperature adaptability, battery life, safety and other properties has greatly improved. The performance of several lithium-ion batteries is shown in Tab. 2. Taking into account the EMU's low temperature performance, service life, safety, and energy density as the main requirements, lithium titanate batteries have become one of the most suitable power sources for use on EMUs today.

Table 2 Lithium - ion battery performance comparison

Index	Lithium manganese oxide	Lithium iron phosphate	Lithium titanate
Energy density (W·h/kg)	120	110	80
Charge and discharge life (Cycle)	1000	6000	6000
Self-discharge rate (%/month)	5	5	5
Memory effect	no	no	no
Environmental pollution	no	no	no
Safety	medium	good	good

3 LITHIUM TITANATE BATTERY MODELING AND SIMULATION

There are three basic battery models, specifically experimental models, electrochemical models, and circuit models. Experimental and electrochemical models are not well suited to represent the battery dynamics of the battery pack for the state of charge (SOC) estimation of the battery pack. However, circuit-based models can be used to represent the electrical characteristics of the battery. The simplest electrical model consists of an ideal voltage source with an internal resistor in series. However, this model does not consider the battery SOC. Another model is based on an open circuit voltage in series with a resistor and a parallel RC circuit, with the so-called Warburg impedance. The identification of all parameters of the model is based on a rather complex technique called impedance spectroscopy. Shepherd developed an equation that describes the electrochemical behavior of a battery based directly on terminal voltage, open circuit voltage, internal resistance, discharge current, and state of charge. This model is not only suitable for discharge but also for charging. However, there is an algebraic cycle problem in the closed-loop simulation of the Shepherd model. Therefore, this paper studies a battery model that only uses SOC as a state variable [13]. This model is very similar to the Shepherd model, but it does not produce algebraic cycle problems and can accurately describe the charge-discharge characteristics of lithium titanate batteries.

3.1 Lithium Titanate Battery Modeling

Since the electrochemical reaction inside the lithium titanate battery is a complex non-linear process, each element in the electrical model is based on a nonlinear equation that includes parameters and battery states. The parameter is the empirical coefficient, which is determined by the battery's own specifications.

The nonlinear battery model is shown in Fig. 2. The main circuit uses a controlled voltage source and resistors in series to sample the output current of the battery. The actual charge and discharge capacity of the battery is obtained through the integration process. The controlled source voltage is then calculated by the equation to achieve the battery output current to the battery. Closed loop feedback of open circuit voltage.

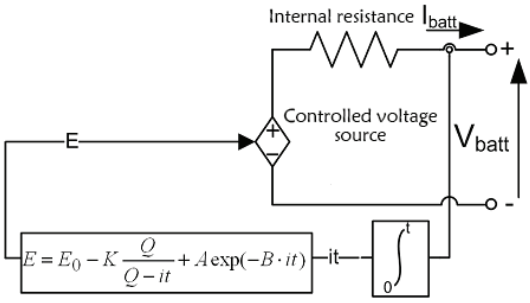

Figure 2 Non-Linear battery model

The controlled voltage source voltage can be described by the following equation:

$$E = E_o - K\frac{Q}{Q - \int i\mathrm{d}t} + A\,exp(-B\cdot\int i\mathrm{d}t) \quad (1)$$

$$V_{batt} = E - R\cdot i \quad (2)$$

where: E - Controlled source voltage (V), E_o - Maximum charge voltage of lithium titanate battery (V), K - polarization voltage (V), Q - Battery capacity (Ah), $\int i\mathrm{d}t$ - Actual charging capacity (Ah), A - Voltage drop in the index area (V), B - The reciprocal of the index area $(\mathrm{Ah})^{-1}$, V_{batt} - Output voltage (V), R- Battery internal resistance (Ω), i- Battery current (A).

3.2 Model Parameter Identification

This model can accurately represent the behavior of many different kinds of batteries, if the parameters are well established. The main feature of this battery model is that parameters can be easily derived from the manufacturer's discharge curve. Fig. 3 shows typical battery discharge characteristics.

Three necessary points for extracting the model parameters (Fig. 3): fully charged voltage, the end of the exponential region (voltage and charge) and the end of the nominal region (voltage and charge). The index part $(A\,exp(-B\cdot it))$ is calculated using the first two points as follows:

Voltage drop in the index area (A, A)

$$A = E_{Full} - E_{Exp} \quad (3)$$

Capacity at the end of the index area (B, A·h)

$$B = \frac{3}{Q_{Exp}} \quad (4)$$

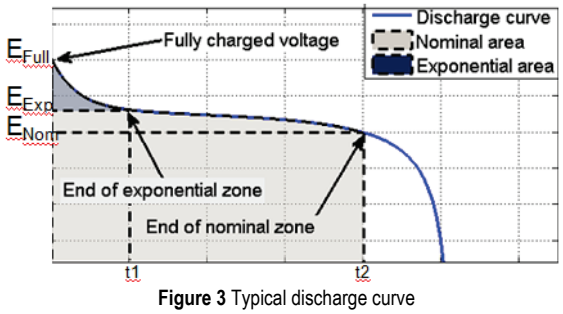

Figure 3 Typical discharge curve

Other parameters can be calculated using Eq. (1). The polarization voltage K can be derived from the full charge voltage (E_{Full}) and the third point (end of the nominal region: Q_{Nom} and E_{Nom}):

$$K = \frac{\left(E_{Full} - E_{Nom} + A(exp(-B\cdot Q_{Nom}) - 1)\right)\cdot(Q - Q_{Nom})}{Q_{Nom}} \quad (5)$$

Finally, the voltage constant E_o can be derived from the full charge voltage.

$$E_o = E_{Full} + K + R\cdot i - A \quad (6)$$

The parameters of the lithium titanate battery used in this paper are shown in Tab. 3.

Tab 3 Lithium Titanate Battery Monomer Parameters

Index	Parameter value
Type of battery	Lithium titanate battery
Battery capacity	10 A·h
Battery capacity Q	2.3 V
Maximum charging voltage	2.8 V
Discharge cut-off voltage	1.5 V
Ohm resistance	<1.2 mΩ
Energy Density	78 W·h/kg
Charge and discharge life	10000

The point-of-settlement curve provided by the battery supplier is shown in Fig. 4.

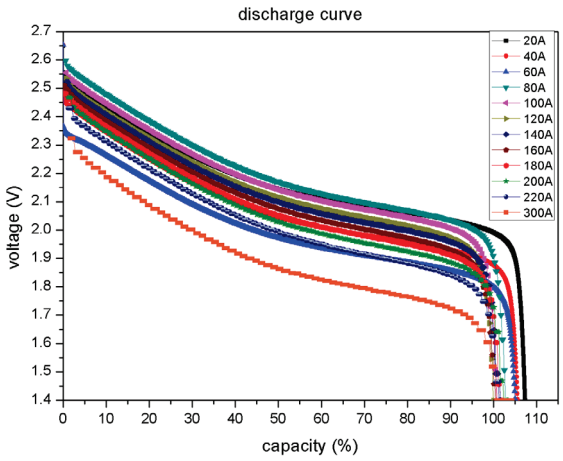

Figure 4 Discharge curve of Lithium Titanate battery

The model parameters can be calculated from the discharge curve and the basic battery parameters as shown in Tab. 4.

Tab 4 Lithium Titanate Battery Model Parameters

Index	Parameter value
E_o	2.8 V
K	0.00876 V
Q	10 A·h
A	0.23 V
B	3.5 $(A·h)^{-1}$
R	0.0052 Ω

Lithium titanate batteries were discharged at different rate currents. The simulated waveforms are shown in the figure below. The green line represents the controlled source voltage E and the blue line represents the battery output voltage V_{batt}. The difference between them is the internal resistance of the battery. The voltage drop.

3.3 LithiumTitanate Monomer MATLAB Simulation

The simulation model built in MATLAB simulation software is shown in Fig. 5.

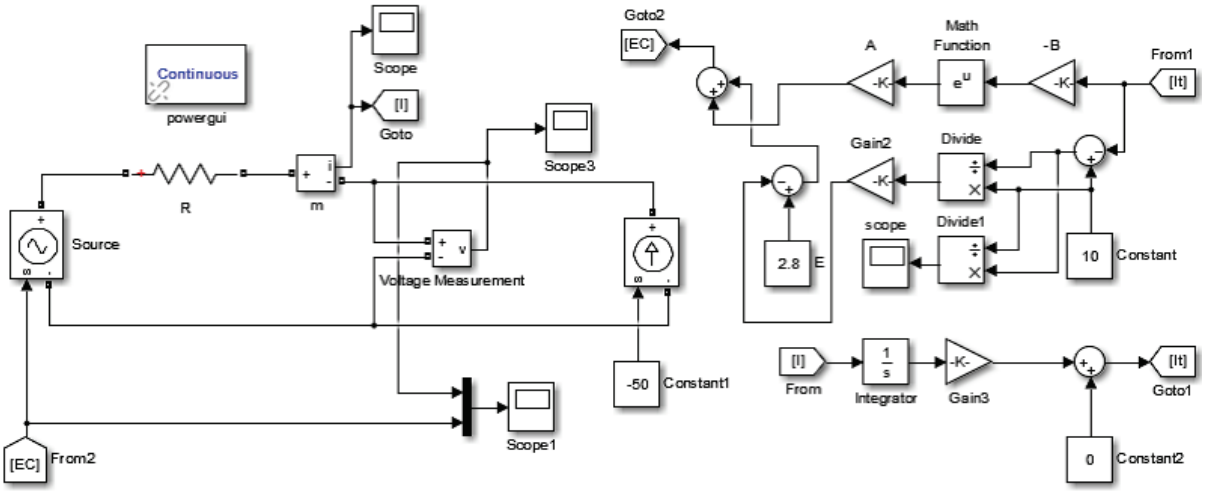

Figure 5 Lithium Titanate Simulation Model

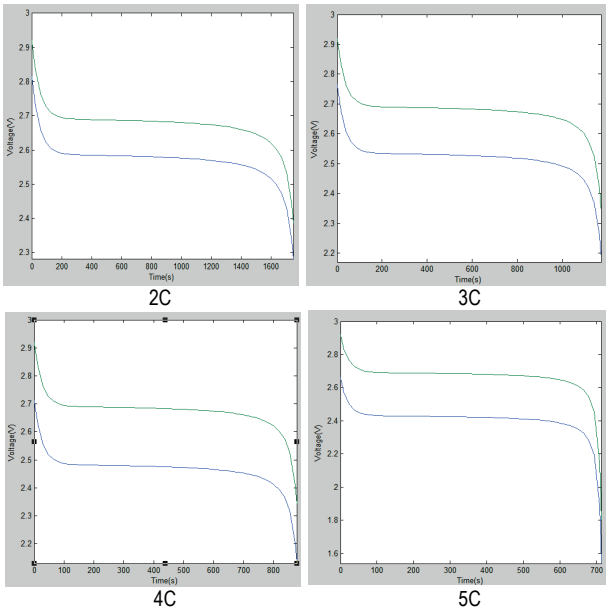

Figure 6 Different magnification discharge current simulation waveform

Comparing the discharge curves at different rates, we can see that the discharge rate of the battery is faster at high rate, which can meet the demand of EMUs for rapid discharge.

3.4 Battery Simulation

Due to the limitation of the capacity of single cell batteries, single cells are often connected in parallel to meet capacity requirements in electric vehicle on-board batteries and power grid energy storage systems. For example, the 2008 Beijing Olympic Games pure electric buses use 104 modules in series, each module consists of 4 Single cell batteries connected in parallel; the BYD Shenzhen headquarters energy storage demonstration system consists of 16 series branches in parallel. Similarly, the batteries need to be connected in series to meet the voltage requirements. In the technical requirements of the EMU battery transfer, the battery pack needs to reach the voltage capacity requirements of 110 V and 240 A·h.

In order to obtain a 110 V battery pack, a lithium titanate battery cell with a rated voltage of 2.3 V needs to be connected in series and in parallel. According to the result of the capacity configuration, the number of series-connected lithium titanate monomers required for the battery string is 45, and the number of parallel-connected battery strings is 24.

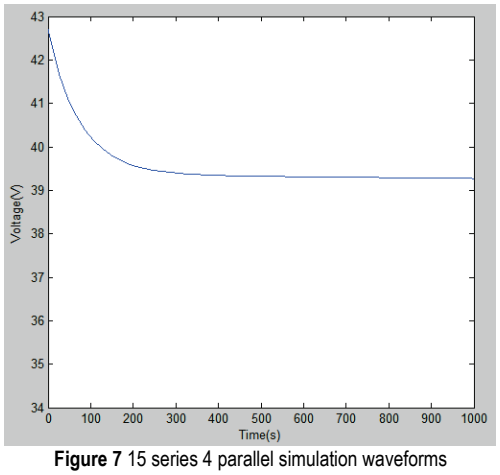

Figure 7 15 series 4 parallel simulation waveforms

The single-unit lithium titanate battery cell was built for series-parallel simulation. For the convenience of research, the first 15 series and 4 small-module simulations were performed, and the resulting output voltage waveforms are shown in Fig. 7.

The 15 series and 4 parallel modules obtained are then connected in series of 3 and 6 in parallel, and the resulting output voltage waveform is shown in Fig. 8

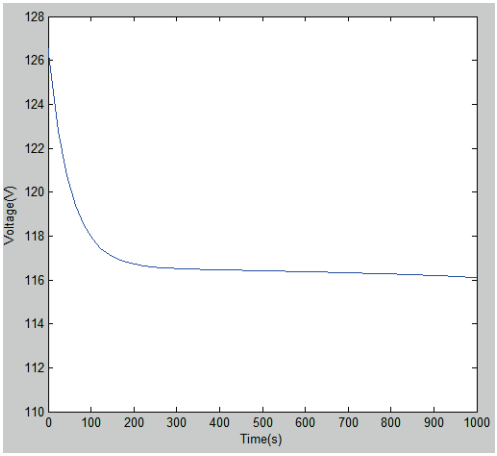

Figure 8 45 series 24 parallel simulation waveforms

From the output voltage simulation waveform, we can see that the 45-series and 24-group combined stable discharge voltage is about 116V, which can meet the requirements of the battery system for the battery system to output 110V DC.

4 BATTERY TRANSFER SYSTEM SIMULATION AND EXPERIMENT

4.1 Simulation Analysis

In MATLAB/Simulink, a co-simulation of a battery transfer system with a standard speed of 250 km/h EMUs is performed. The simulation model is shown in Fig. 9.

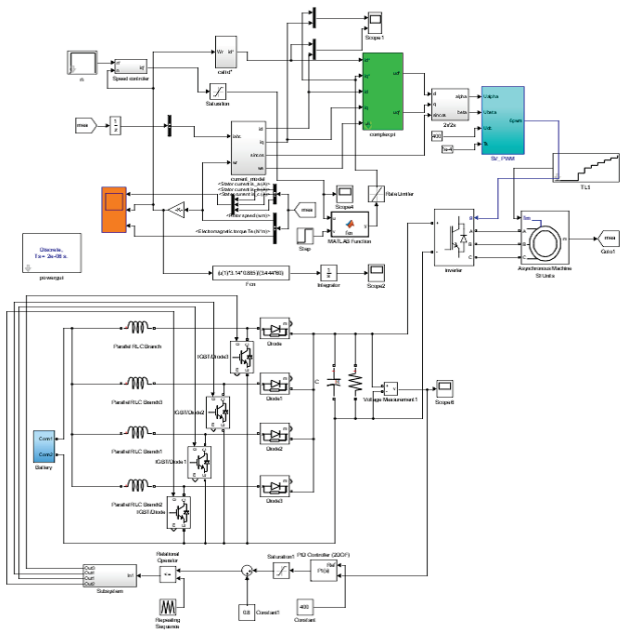

Figure 9 Simulation model of battery self-shifting driven system

Based on the basic parameters of the EMUs with a standard speed of 250 km/h, the gear ratio is 3.444, the transmission efficiency is 0.975, and the wheel diameter is 920 mm. It is calculated that the motor speed is 100 rpm at a vehicle speed of 5 km/h. According to the actual situation, the EMU's torque is 1045 N·m when running at 5km/h, so the given motor torque is 1045 N·m in the simulation process. Fig. 10 shows the motor current, speed, and torque simulation waveforms for 5 km/h operation.

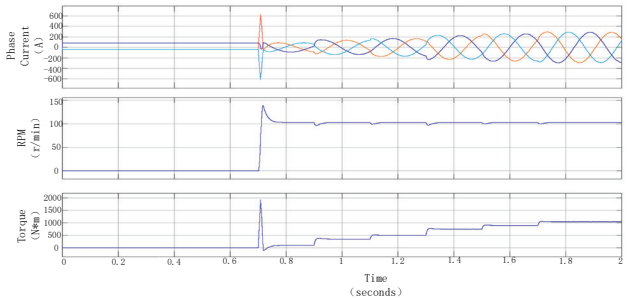

Figure 10 Simulation waveforms of phase current, speed and torque at 5 km/h

In order to avoid the sudden increase of the load caused by the current overcurrent, the torque is increased in a segmented manner. From the figure above, it can be seen that the designed battery shift system can quickly reach the given torque requirement, and the load change resistance during the loading process is relatively low. It is good.

At a running speed of 10km/h, the motor speed is 200 rpm and the given torque is 994 N·m. The simulation waveform obtained is shown in Fig. 11. It can be seen that the motor can still reach the given speed at the speed of 10km/h. The requirements of the moment and the characteristics are good, and it can be verified that the scheme of the battery transfer system designed in this paper is still valid at a speed of 10 km per hour.

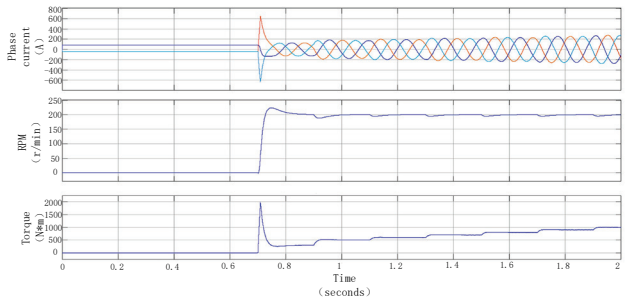

Figure 11 Simulation waveforms of phase current, speed and torque at 10 km/h

4.2 Experimental Verification

(a) 5 km/h simulation operation experiment

When the battery is fully charged, the traction inverter is powered by a DC/DC converter and the traction inverter pulls the load of the asynchronous motor. The output voltage is between DC 400V ± 50V and the motor speed reaches 100 rpm ± 5 rpm. The torque is 1045 N·m. Under this operating condition, it continuously operates until the DC conversion device reports under voltage. Fig. 12 shows the waveform of the intermediate DC current, intermediate voltage, and speed at 5 km/h.

The experiment was started at time 26'28", and the traction system working time, battery voltage, output current, and remaining battery capacity were recorded at

regular intervals. Tab. 5 shows the actual test data for a 5 km/h experiment.

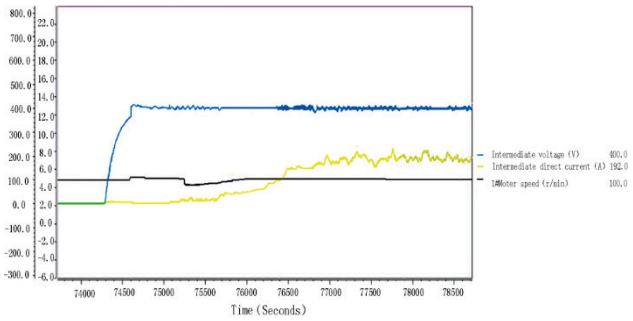

Figure 12 Waveforms of 5 km/h simulation operation

Table 5 Experimental data of 5 km/h simulation operation

Time	Voltage /V	Current /A	SOC /%
26'28"	111.8	344.5	97
28'00"	109.6	355.2	92
29'00"	108.6	357.6	89
31'55"	105.5	369.3	81
33'44"	103.8	378.2	75
35'08"	102.7	383.8	70
38'07"	100.7	390.9	61
40'27"	99.1	404.8	53
42'53"	97.2	405.8	45
45'17"	95.5	408.0	37
48'03"	93.4	434.8	27
49'59"	91.6	440.3	20
51'34"	88.6	430.4	14

From the analysis of the data, it can be seen that from the 26'28" experiment to the 51'34" battery discharge deadline, the system has been running for about 25 minutes, and the distance traveled at 5km/h is km, far more than the battery shift. The expected goal of the system moving 100 m verified the correctness and feasibility of the designed battery shift system.

(b) 10 km/h simulation operation experiment

The 5 km/h simulated running test has verified that the battery shift system designed can meet the expected requirements. Now the simulation running experiment with the speed of 10 km/h is performed to observe the running performance of the system after the speed increase.

When the battery is fully charged, the traction inverter is powered by a DC/DC converter and the traction inverter pulls the load of the asynchronous motor. The output voltage is between DC 400V±50V and the motor speed reaches 200 rpm±5 rpm. The torque 994 N·m continues to work under this condition until the DC conversion device reports an undervoltage. The waveforms of intermediate DC current, intermediate voltage, motor speed, and motor torque at 10 km/h are shown in Fig. 13.

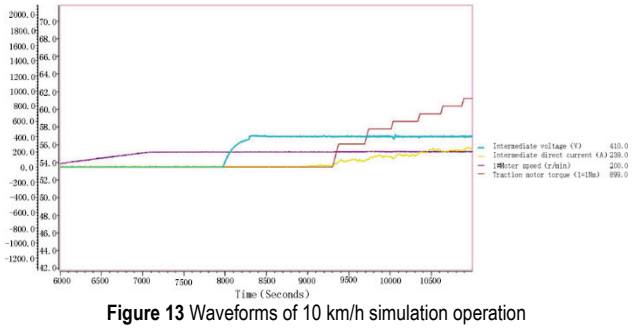

Figure 13 Waveforms of 10 km/h simulation operation

Table 6 Experimental data of 10 km/h simulation operation

Time	Voltage /V	Current /A	SOC /%
37'15"	116.7	536	98
38'21"	109.5	565	93
39'45"	106.4	580	88
41'05"	104.9	599	80
42'22"	103.5	617	76
43'08"	102.9	616	70
44'06"	101.4	619	63
45'10"	100.6	620	57
47'21"	97.8	655	47
48'37"	95.8	661	39
49'53"	93.0	678	22
50'25"	90.8	707	19
51'42"	88.9	718	11

From the analysis of the data, we can see that from the 37'15" experiment to the 51'42" battery discharge deadline, the system has been running for about 14 minutes. The distance traveled at 10 km/h is km, which can be verified in this paper. The battery transfer system solution is still valid at 10 km/h.

5 CONCLUSION

In this paper, a lithium titanate battery model that satisfies the requirement of moving trains is studied under the background of battery transfer technology. Lithium titanate monomer simulation and battery pack simulation were mainly performed. The dynamic model was adopted in the single element simulation to consider the influence of the nonlinear characteristics and state of the lithium titanate battery on the battery. The dynamic discharge process of the lithium titanate battery was studied through the closed-loop feedback of the output current on the open circuit voltage. In the battery pack simulation, the lithium battery cells are connected in series and parallel. The simulation results show that this scheme can meet the requirements of the battery system for the battery system to output 110V DC. Completed is the overall simulation analysis and experimental verification of the EMU battery transfer system.

Acknowledgements

This work was financially supported by the Fundamental Research Funds for the Central Universities (2017JBM060) and National Key R&D Program of China (2016YFB1200601-B22).

6 REFERENCE

[1] Zhang, S. S., Xu, K., & Jow, T. R. (2006). Charge and discharge characteristics of a commercial LiCoO2-based 18650 Li-ion battery. *Journal of Power Sources*, 160, 1403-1409. https://doi.org/10.1016/j.jpowsour.2006.03.037

[2] Liu, H., Wang, L. & Gao, X. R. (2004). Current situation and prospects of the detection technology for the contact-loss of pantograph on electric locomotive. *Locomotive & Rolling Stock Technology,* 49(7), 1151-1159. https://doi.org/10.3969/j.issn.1007-6034.2004.06.001

[3] Feng, X., Wang, L. J., & Ge, X. L. (2008). Research and simulation on traction and drive control system of high-speed EMU. *Electric Drive, 38*(11), 25-28. https://doi.org/10.3969/j.issn.1001-2095.2008.11.006

[4] Yang, S. B. & Wu, M. L. (2010). Study on harmonic distribution characteristics and probability model of high

speed EMU based on measured data. *Journal of the China Railway Society, 32*(3), 33-38. https://doi.org/10.3969/j.issn.1001-8360.2010.03.006

[5] Shepherd, C. M. (1965). Design of Primary and Secondary Cells - Part 2. An equation describing battery discharge. *Journal of Electrochemical Society*, 112, 657-664. https://doi.org/10.1149/1.2423659

[6] Mauracher, P. & Karden, E. (1997). Dynamic modelling of lead/acid batteries using impedance spectroscopy for parameter identification. *Journal of Power Sources, 67*(1-2), 69-84. https://doi.org/10.1016/S0378-7753(97)02498-1

[7] Bauman, J. & Kazerani, M. A. (2008). A Comparative Study of Fuel-Cell–Battery, Fuel-Cell–Ultracapacitor, and Fuel-Cell–Battery–Ultracapacitor Vehicles. *IEEE Transactions on Vehicular Technology*, 57(2), 760-769. https://doi.org/10.1109/TVT.2007.906379

[8] Rodrigues, S., Munichandraiah, N., & Shukla, A. K. (2000). A review of state-of-charge indication of batteries by means of ac impedance measurements. *Journal of power Sources, 87*(1), 12-20. https://doi.org/10.1016/S0378-7753(99)00351-1

[9] Windarko, N. A., Choi, J. & Chung, G. B. (2011). SOC estimation of LiPB batteries using Extended Kalman Filter based on high accuracy electrical model. *IEEE International Conference on Power Electronics & Ecce Asia,* 2015-2022. https://doi.org/10.1109/ICPE.2011.5944483

[10] Plett, G. (2002). LiPB dynamic cell models for Kalman-filter SOC estimation. *The 19th International Battery, Hybrid and Fuel Electric Vehicle Symposium and Exhibition (EVS-19)*, Busan, Korea, October 19-23.

[11] Kim, G. H. & Pesaran, A. A. (2006). Battery thermal management system design modeling. *The 22nd International Battery, Hybrid and Fuel Cell Electric Vehicle Conference and Exhibition (EVS-22)*, Yokohama, Japan October 23-28.

[12] Chen, B., Gao, Y., Ehsani, M., & Miller, J. M. (2009). Design and control of an ultracapacitor boosted hybrid fuel cell vehicle. *In Proc. IEEE Vehicle Power and Propulsion Conf. VPPC '09*, Dearborn, MI, USA, September 7-10, 696-703. https://doi.org/10.1109/VPPC.2009.5289783

[13] Bellman, R. (1966). Dynamic Programming. *Science, 153*(3731), 34-37. https://doi.org/10.1126/science.153.3731.34

Contact information:

Liwei ZHANG, Associate Professor
(Corresponding Author)
Beijing Jiaotong University
No. 3 Shangyuancun,
Haidian District, Beijing 100044, China
E-mail: lwzhang@bjtu.edu.cn

Wenyan DONG, Master Candidate
Beijing Jiaotong University
No. 3 Shangyuancun,
Haidian District, Beijing 100044, China
E-mail: 16121432@bjtu.edu.cn

Yang YANG, Master Candidate
No.6, north section 2, zhongguancun,
Haidian District, Beijing 100080, China
E-mail: 15121495@bjtu.edu.cn

Minghe SUN, Doctoral Candidate
Beijing Jiaotong University
No. 3 Shangyuancun,
Haidian District, Beijing 100044, China
E-mail: mhsun@bjtu.edu.cn